Journal of Applied Polymer Science

Enhancement of polyaniline properties by different polymerization temperatures in hydrazine detection

Kavirajaa Pandian Sambasevam, Sharifah Mohamad, Sook-Wai Phang
Department of Chemistry, Faculty of Science, University of Malaya, 50603 Kuala Lumpur, Malaysia
Correspondence to: S.-W. Phang (E-mail: pinkyphang@gmail.com)

ABSTRACT: In this study, a simple and cost effective chemical sensor for hydrazine detection was developed using polyaniline (PAni). PAni was synthesized via chemical oxidative method at different polymerization temperatures (−10, −5, 0, and 25°C) in the presence of sodium dioctyl sulfosuccinate (AOT) as dopant. The effect of polymerization temperature on the performance of the PAni sensor for hydrazine detection was evaluated. The sensor response was analyzed using UV–Vis spectrometer, where there is notable decrease in polaron peak at ~780 nm after the PAni was exposed to hydrazine. The reduction in the polaron peak is attributed to the decrease in the conductivity of PAni thin films owing to dedoping process by hydrazine. Fourier transform infrared analysis was carried out to study the intensity ratio of quinoid/benzenoid peak to identify the changes in chemical structure of PAni upon exposure to hydrazine. Besides that, all PAni sensors synthesized at different polymerization temperatures showed good reusability up to 10 cycles with respond and recovery time of 0.12 min and 0.08 min, respectively. Data collected in this study indicate that PAni which was synthesized at −5°C could act as sensitive sensor for hydrazine detection with a detection limit of 0.24 ppm. © 2014 Wiley Periodicals, Inc. J. Appl. Polym. Sci. **2015**, *132*, 41746.

KEYWORDS: addition polymerization; conducting polymers; properties and characterization; sensors and actuators

Received 10 July 2014; accepted 7 November 2014
DOI: 10.1002/app.41746

INTRODUCTION

In recent years, conducting polymers have gained much attention due to their versatile applications in electronic devices, light emitting diodes, sensors, actuators, corrosion protection coatings, and microwave absorption.[1–5] Among the conducting polymers, polyaniline (PAni) is one of the promising semiconductors due to its ease of synthesis,[6] high conductivity, low production cost, and good environmental stability.[7,8] However, some of the known disadvantages of PAni include low molecular weight and having many defect sites when it was synthesized at room temperature. These disadvantages could be critical as the defect sites and low molecular weight could significantly depreciate the mechanical and electrical properties. Fortunately, the disadvantages can be overcome by manipulating the polymerization temperature. There are several studies on the synthesis of PAni at sub-zero temperature that reported great improvements in the molecular weight and structure of the PAni. However, most of these improved PAni were being synthesized in the powder form which restricts its application in the field of sensing technology.[6,8]

Sensor is one of the crucial analytical technologies and tools in detecting toxic chemicals in the environment. Hydrazine and its derivatives are commonly known for fuels in explosives, antioxidants, rocket propellants, blowing agents, photographic chemical, corrosion inhibitor, insecticides, and plant growth regulators.[9] Nevertheless, hydrazine is well known as neurotoxin, carcinogen, mutagen, and hepatotoxic.[10] Besides that, exposure to high level of hydrazine can cause irritation to nose, eye, throat, dizziness, nausea, temporary blindness, pulmonary edema, and coma, which will eventually endanger the liver, kidneys, and central nervous system of humans.[11]

Therefore, there is the need to have an effective and sensitive method for hydrazine detection. Presently, several efforts have been made in developing rapid, sensitive, and selective methods for detection of hydrazine. The methods include using different metal oxides, electrodes, and semiconductors.[12,13] Electroanalytical technique is a direct and effective method for detection of hydrazine.[14] Unfortunately, hydrazine exhibits irreversible oxidation which requires large overpotential at bare carbon electrodes. Recently, various chemically modified electrodes (CMEs) have been prepared and applied in the detection of hydrazine.[15–19] The modifications were able to significantly lower the overpotential and increase the oxidation current response. However, the tedious preparation method and expensive electrode modification techniques have made this method cumbersome, and many are still finding for an alternative methodology. The preference for a

Additional Supporting Information may be found in the online version of this article.

conducting polymer especially PAni over a conventional metal as sensing material stems from several advantages such as it can be operated at lower applied voltages and temperatures, unique acid-base chemistry, and it interacts more favorably with both organic and inorganic compounds.[20]

In this work, PAni were synthesized via chemical oxidation method at different polymerization temperatures to optimize its sensing performance by having higher molecular weight PAni with lesser defect sites. The performance of the PAni sensor was evaluated using ultraviolet-visible (UV-Vis) and supported by standard four probe method (conductivity studies) and Fourier transform infrared (FTIR) spectrometer.

EXPERIMENTAL

Chemicals

Chemicals such as aniline (Ani) monomer, dioctyl sodium sulfosuccinate (AOT) dopant, ammonium peroxydisulfate (APS), and lithium chloride (LiCl) were purchased from Sigma Aldrich and used as received. Hydrochloric acid (HCl) 37% and analytical grade toluene were purchased from Lab Scan Sdn. Bhd. and Starform Sdn. Bhd., respectively. Distilled water was used throughout the research. All the chemicals and reagents were used without purification unless noted.

Synthesis

PAni was synthesized via chemical oxidation method at 25°C. First, 1 mmol of AOT was dissolved in 1*M* of HCl followed by the dropwise addition of 1 mmol of Ani. Then, 15 mmol of APS solution was slowly added into the solution mixture and the polymerization was allowed to continue for 24 h. After that, the product, PAni was washed with distilled water for three times and subsequently dissolved (3 wt %) in toluene. Then, PAni solution in toluene was deposited on a well-cleaned glass substrate prior to spin coating technique. This was done in a three-step process (acceleration for 10 s at 1000 rpm, steady-state coating for 10 s at 5000 rpm followed by deceleration for 10 s at 1000 rpm) on a spin coater (Model: Spin 150, Germany). This technique yielded PAni thin film with a uniform coating, and it was subjected to 30 min drying in oven to remove remaining toluene solvent from the thin film. The same approach was used to synthesize PAni at −5, −10, and 0°C. PAni at 0°C was synthesized in ice bath. For synthesis at sub-zero temperature (−5 and −10°C), optimized amount of LiCl was added to prevent the freezing of PAni reaction mixture.

Characterizations

The characterizations of PAni films were carried out using FTIR (Perkin Elmer RX1 FT-IR ATR) spectrometer in the range of 400–4000 cm^{-1} and UV-Vis (UV-1650 PC) spectrometer in the range of 300–900 nm. X-ray diffraction patterns were obtained using Empyrean X-ray diffractometer (XRD), equipped with a Cu target at 40 kV and 40 mA. The measurements were performed within a 2θ range of 5–80° at scan speed of 2°/min. Conductivity characterization were performed by using four point probe, Loresta HP in the conductivity range of 10^{-7} to 10^{7} S/cm.

Set-up for PAni Thin Film in Hydrazine Detection

PAni film was immersed in hydrazine solution (1–100 ppm) in cuvette cell to determine the response of PAni against hydrazine as shown in Supporting Information Figure S1. The measurements were taken before and after immersion into hydrazine solution using UV–Vis, standard four point probe, and FTIR spectrometer.

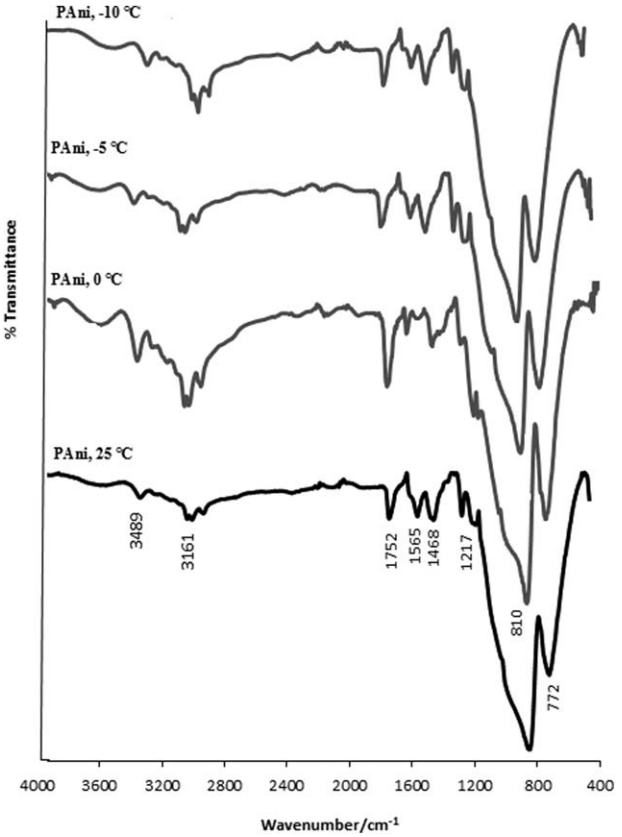

Figure 1. FTIR spectra of PAni synthesized at various polymerization temperatures.

RESULTS AND DISCUSSION

Characterizations

Figure 1 shows the FTIR spectra of PAni synthesized at different polymerization temperatures (−10, −5, 0, and 25°C). All PAni showed a broad transmission band at wavenumbers higher than 2000 cm^{-1} which is the typical form of conducting PAni.[21,22] The bands observed in the range of 2800–3600 cm^{-1} are attributed to the H-bonding to the adjacent molecules in PAni chains. Typically, the bands observed at 3161 cm^{-1} and 3489 cm^{-1} belong to the N—H stretching and O—H stretching, respectively.[23] The band at 1752 cm^{-1} corresponds to the C═O which arose from the AOT dopant.[24] Meanwhile, peaks at 1565 cm^{-1} and 1468 cm^{-1} contributed to the stretching vibration mode of quinoid and benzenoid rings, respectively, which are characteristic peaks of conducting PAni.[25] A characteristic band at 1217 cm^{-1} was found to be the feature of conducting protonated form, and it is interpreted as a C—$N^{+\bullet}$ stretching vibration in the polaron structure.[26] The lower region such as 900–700 cm^{-1} represents the aromatic ring and out-of-plane deformation vibrations. Typically the band at 810 cm^{-1} is attributed to C—C and C—H stretching for the benzenoid unit of PAni.[27] In general, FTIR spectra of PAni synthesized at

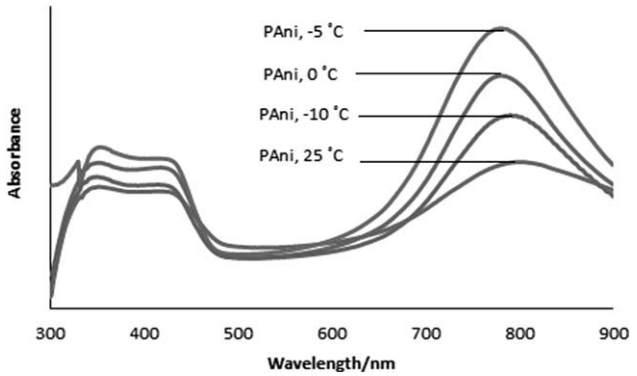

Figure 2. UV–Vis spectra of PAni synthesized at various polymerization temperature.

various polymerization temperatures exhibit identical characteristic bands in the range of 400–4000 cm^{-1}.

Figure 2 shows the UV–Vis absorption spectra of PAni synthesized at different polymerization temperatures (−10, −5, 0, and 25°C). Typically, all PAni spectra have shown three characteristic peaks at ~340–350 nm, ~426–433 nm, and ~775–786 nm. The absorption peak at ~340–350 nm arose from π–π^* transition of the benzenoid rings, while the peaks at ~426–433 nm and ~775–786 nm are attributed to the polaron–π^* and π–polaron transitions, respectively.[28–32] In addition, the peaks at ~426–433 nm and ~775–786 nm can be related to the doping level and formation of polarons.[29,30] According to Xia and Wang, the extent of doping level can be estimated from the absorbance ratio of ~775–786 nm (π–polaron) to ~~340–350 nm (π–π^* transition), where the higher the absorbance ratio value, the higher is the doping level in the PAni emeraldine salt structure.[32] Table I shows the UV–Vis characteristic peak assignments and absorbance ratio of PAni synthesized under different polymerization temperatures. The results indicate that PAni, −5°C possess the highest degree of doping extension, followed by PAni, 0°C, PAni, −10°C, and PAni, 25°C. Even though PAni, −10°C was synthesized at the lowest sub-zero temperature, the addition of LiCl in excess during the polymerization to prevent the freezing of reactants could have adversely affect the PAni, −10°C structure which caused ring chlorination and reduced the degree of doping.[33] As for the PAni, 25°C presumably the high number of defect sites and less polarons throughout the PAni chains has led to reduction in the degree of doping.[34]

In this study, X-ray diffractogram of PAni synthesized at different polymerization temperatures is shown in Figure 3. In general, crystallinity and predilection of conducting polymers with

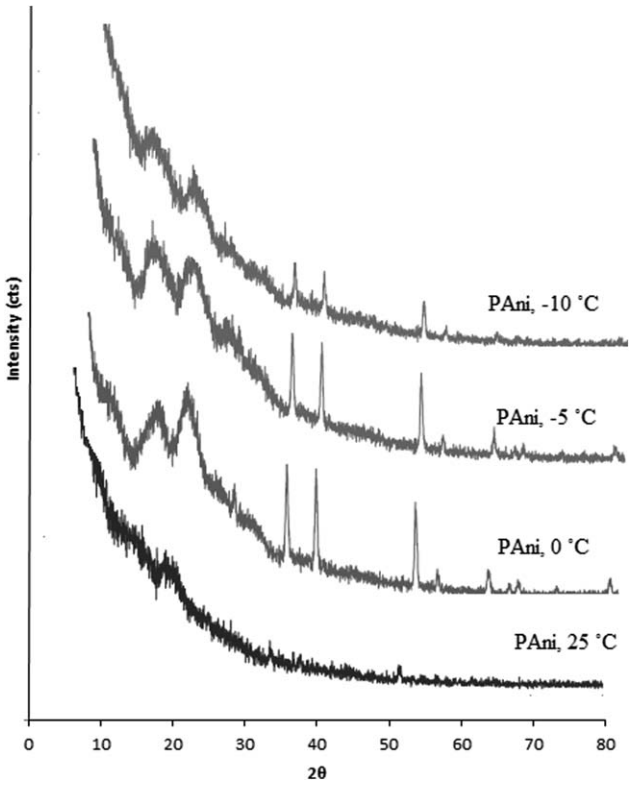

Figure 3. XRD of PAni synthesized at different polymerization temperatures.

Table II. Conductivities of PAni Synthesized at Various Polymerization Temperatures

PAni	Conductivity (S/cm)
PAni, −10°C	0.232
PAni, −5°C	1.813
PAni, 0°C	0.816
PAni, 25°C	0.006

highly ordered system could display a metallic-like conductive state.[35] Sharp peaks at $2\theta = 35°$, 40°, and 53° are visible only in PAni, −10, −5, and 0°C. Therefore, it indicates that the degree of crystallinity is related to molecular weight.[36] Similar phenomenon observed by Stejskal and his coworkers, that as the polymerization temperature decreases, it increases the molecular weight of PAni. While the molecular weight reflects the macromolecular structure of PAni, it improves the degree of

Table I. The Assignments of UV–Vis Absorption Peaks for PAni Synthesized at Various Polymerization Temperatures

Sample	π–π^* transition (nm)	Absorbance	π–polaron transition (nm)	Absorbance	Absorbance ratio $A_{775-786}/A_{340-350}$
PAni, −5°C	350	0.775	786	1.351	1.743
PAni, 0°C	340	0.627	775	1.019	1.625
PAni, −10°C	347	0.550	779	0.847	1.540
PAni, 25°C	340	0.533	782	0.663	1.244

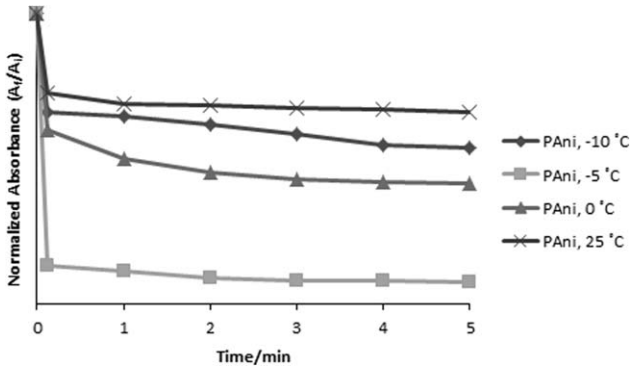

Figure 4. Normalized absorbance responses of PAni in hydrazine detection (1 ppm) against time in terms of UV–Vis investigation.

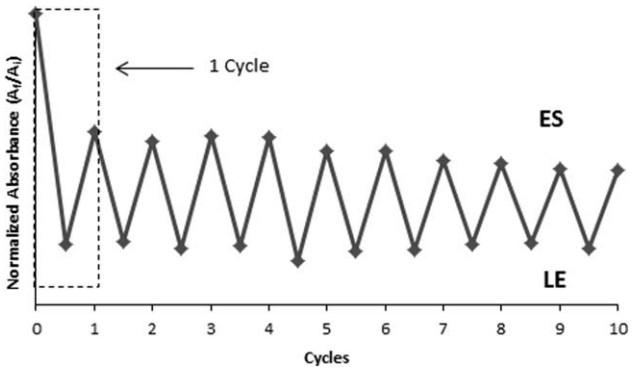

Figure 6. Reusability study of PAni upon dedoping by hydrazine and redoping by HCl.

crystallinity that associated with the supramolecular structure.[37] Figure 3 exhibits two broad peaks in the range of 2θ angles 14–17° and 18–23° which are similar to those of the PAni reported elsewhere.[38,39] These peaks arose due to the repetition units of regular aniline monomers, and it indicates the densely packed phenyl rings which rise to a planar conformation. Besides that, there is another broad peak centered on $2\theta = 20$–21° which is obtained from the AOT dopant. The results show that all the resulting PAni is in the form of highly doped emeraldine salt.[40,41] The obtained X-ray diffractogram is well supported by the conductivity characterization as shown in Table II.

The conductivity of PAni synthesized at various polymerization temperatures are shown in Table II. PAni, −5°C recorded the highest conductivity (1.813 S/cm), followed by PAni, 0°C, PAni −10°C, and PAni 25°C with conductivities of 0.816, 0.232, and 0.006 S/cm, respectively. The conductivity of PAni depends on the degree of doping, oxidation state, and molecular weights.[42] PAni, −5°C that was synthesized at sub-zero temperature may possess less defect sites, high crystallinity, and long polymer chain with numerous polarons and maximum inter or intra-chain interactions which resulted in high conductivity.[37] Besides that, according to Table I, absorbance ratios ($A_{775–786}/A_{340–350}$) of PAni synthesized at different polymerization temperatures are in good agreement with the degree of doping extension in PAni chains that explains conductivity behavior of PAni as discussed earlier.

UV–Vis Sensor Measurements

Effect of Response Time. PAni synthesized at different polymerization temperatures (−10, −5, 0, and 25°C) were used as sensors to detect 1 ppm of hydrazine at different time intervals. Figure 4 demonstrates the UV–Vis responses of all different polymerization temperatures of PAni against time for 1 ppm of hydrazine. The *y*-axis is the normalized absorbance (A_f/A_i), where A_i is the initial absorbance at polaron peak (~775–786 nm) of the PAni before immersion in hydrazine while A_f is the time-dependent absorbance of the PAni after exposed to hydrazine. In general, all PAni synthesized at different polymerization temperatures showed decrease in normalized absorbance upon exposure to 1 ppm of hydrazine. PAni −5°C exhibits the most significant decrease in normalized absorbance compared to other PAni thin films (−10, 0, and 25°C). The decrease in normalized absorbance of PAni upon exposure to hydrazine is mainly due to the dedoping of PAni by the hydrazine (reducing agent) to change the emeraldine salt (ES) of PAni to be the leucoemeraldine (LE).[43]

Effect of Hydrazine Concentration. Figure 5 shows the response of PAni synthesized at various polymerization temperatures against different hydrazine concentrations (1–100 ppm).

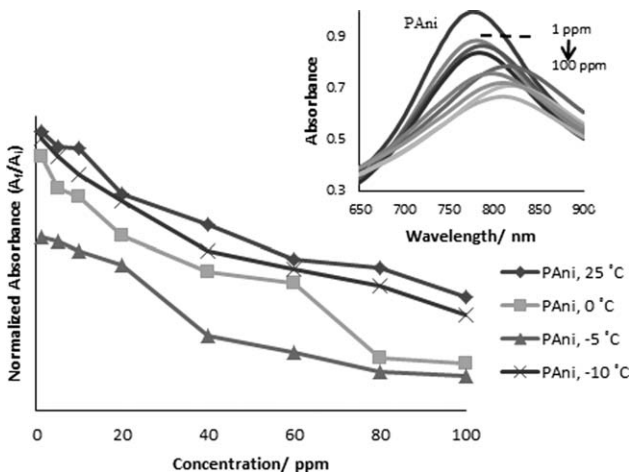

Figure 5. Normalized absorbance responses of PAni against different concentrations of hydrazine (1–100 ppm). (Inset: Absorbance of PAni before and after immersion in hydrazine).

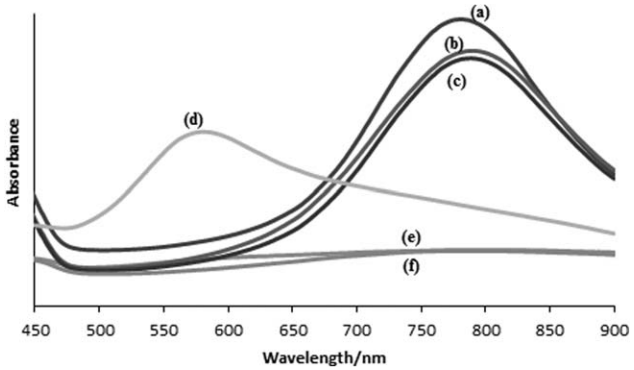

Figure 7. Selectivity study of (a) PAni, −5°C and its immersion in (b) 2-propanol, (c) formic acid, (d) sodium hydroxide, (e) combination of hydrazine and interfering species and (f) hydrazine.

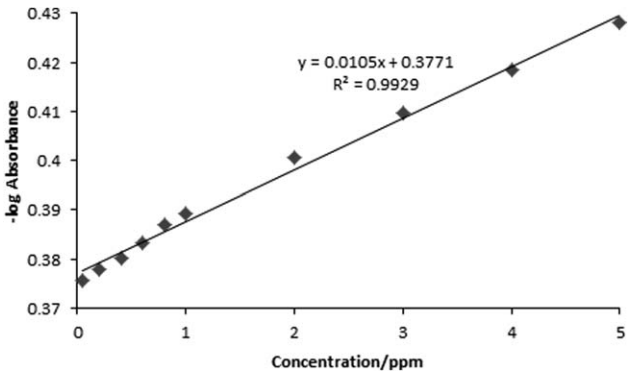

Figure 8. Calibration curve for PAni, −5°C thin film in a linear concentration range from 0.05 to 5.00 ppm.

All the PAni thin film experience reduction in normalized absorbance (A_f/A_i) when immersed in hydrazine solution. The reduction becomes more apparent when higher concentration hydrazine solution was used. This is not totally unexpected as the solution with high concentration of hydazinium ions could easily dedope the PAni ES and consequently reduces the number of polarons from PAni backbone which resulted in significant decrease in polaron intensity, as shown in the inset of Figure 5.[43]

Reusability Study. Since, PAni, −5°C thin film has shown sensitive detection toward hydrazine, it has been chosen to study the reusability and selectivity of PAni, −5°C sensor. The reusability of PAni, −5°C thin film was investigated using UV–Vis spectrometer. ES possesses polarons (free moving electrons) that can be dedoped by hydrazine to form LE with predominating benzenoid units that will record the lowest possible absorbance value at polaron peak (∼780 nm), and LE can be redoped back by an acid to reproduce ES that will increase polaron peak absorbance.[43] The conversion between ES and LE of PAni, −5°C is reversible and can be promoted with the help of reducing agent (hydrazine) and oxidizing agent (acid).[44] Figure 6 shows normalized absorbance values for the reusability study undertaken on PAni with 1 ppm hydrazine and 1*M* HCl. ES showed the highest absorbance at ∼780 nm, and the absorbance decrease during the hydrazine detection. Then LE redoped with HCl acid and the absorbance increased but it never attained the initial absorbance value of ES. Presumably the heavy reaction products did not leave the interface of polyaniline backbone immediately after the reaction.[45,46] The response of PAni, −5°C thin film after immersion in 1 ppm hydrazine was recorded at 7 s while redoping measurement was taken in 5 s after immersion in 1*M* HCl. The PAni, −5°C thin film showed good reusability up to 10 cycles.

Selectivity Study. The ability of a chemical sensor to differentiate the target species in the presence of other species is known as selectivity.[46] In this study, selectivity measurement was performed by using UV–Vis spectrometer since PAni, −5°C can exhibit peaks at different wavelengths according to the nature of reacting species (acid, base, reducing agent, oxidizing agent).[28] Since, hydrazine is a weak base and strong reducing agent, these characteristic have been used to select other interfering species such as sodium hydroxide (base), 2-propanol (reducing agent), and formic acid (reducing agent). Figure 7 shows the UV–Vis spectra of (a) PAni −5°C and its spectra after immersion in (b) 2-propanol, (c) formic acid, (d) sodium hydroxide, (e) combination all interfering species with hydrazine, and (f) hydrazine. The wavelength shift was focused in the region of 450–900 nm only. From the UV–Vis spectra, PAni −5°C has formed a strong absorption peak at 578 nm upon immersion in sodium hydroxide. As we know, PAni −5°C (ES) will change into its emeraldine base (EB) form upon interaction with base which will yield absorption peak in the range of ∼550–580 nm. On the other hand, significant decrease in the absorbance of polaron peak is expected upon the interaction of PAni with reducing agents.[28] Figure 7 clearly shows that, such a significant decrease at polaron peak absorbance was obvious for (f) hydrazine compare to interfering species (reducing agent) such as (b) 2-propanol and (c) formic acid where it showed 13% and 15% of changes from the original PAni −5°C spectrum. Meanwhile Figure 7(e) showed the combination of all analytes in the sensing environment which exhibited a peak with 54% changes that is almost similar to (f) hydrazine detection peak with 55% of changes from the initial absorbance of PAni −5°C. Therefore, PAni −5°C showed good selectivity in the hydrazine detection compare to other base reagents and reducing agents.

Determination Study. Figure 8 shows calibration plot of −log Absorbance against different concentrations of hydrazine from 0.05 to 5.00 ppm. In this case, −log Absorbance was used to obtain positive gradient (slope) in the calibration plot. It can be

Table III. Comparison of the Proposed Sensor for Hydrazine Detection with Some Sensors Reported in Literature for Determination of Hydrazine

Sensor for hydrazine detection	LR[a] (ppm)	LOD[b] (ppm)	Ref.[c]
Cobalt phthalocyanine	4.00–31.00	2.00	[47]
Nickel hexacyanoferrate	12.00–128.00	3.00	[50]
Para-dimethylaminobenzaldehyde	2.00–40.00	1.00	[51]
Zinc oxide nanorod	0.0096–9.60	16.5	[52]
Polyaniline/graphene	0.00032–3.21	493.00	[53]
Polyaniline (PAni, −5°C)	0.05–5.00	0.24	This work

[a] Linear range.
[b] Limit of detection.
[c] References.

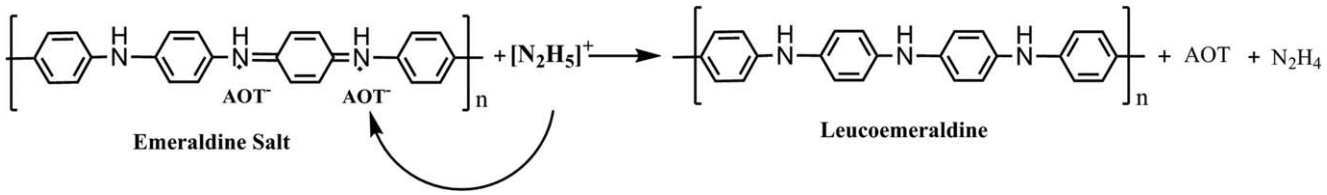

Scheme 1. Schematic representation of the interaction between PAni and hydrazinium ions $[N_2H_5]^+$.

seen from the Figure 8 that the −log Absorbance response increase linearly as the concentration of hydrazine increased. This method exhibits good linear regression equation of $y = 0.0105x + 0.3771$ with a correlation coefficient of 0.9929. The limit of detection (three times the standard deviation of blank/slope of the calibration plot)[47] obtained was 0.24 ppm, which is lower than Occupational Safety and Health Administration (OSHA) standard (1 ppm),[48] meanwhile limit of quantification (10 times the standard deviation of blank/slope of the calibration plot)[49] was 0.82 ppm. The repeatability of the data obtained with PAni, −5°C thin film was tested in 0.5 ppm and 1.0 ppm of hydrazine with a series of 10 measurements, and the relative standard deviation resulted to be 0.25% and 0.22%, respectively which showed that the precision of the proposed sensor material for hydrazine detection is good.

A comparison between proposed sensor (PAni, −5°C thin film) and other sensors for the determination of hydrazine are presented in Table III. For instance, the reported sensors need to undergo tedious preparation steps, expensive electrode modifications, and complicated setups meanwhile PAni, −5°C thin film can be synthesized in bulk and can be spin coated into many thin films in terms of production and moreover, the monomers for synthesis of polyaniline is considerably cheaper than the inorganic particles that reported elsewhere.[50,51] Besides that, the proposed method has better or comparable limit of detection and linear range of concentration values compared with a variety of materials reported in literature for the determination of hydrazine.

Conductivity Measurement

In this study, sensor measurements of PAni with different polymerization temperatures have been further investigated in terms of conductivity and FTIR measurements to understand the interactions occurred between PAni and hydrazine. Thus, response of all PAni synthesized at different polymerization temperatures against different concentrations of hydrazine as a function of conductivity is shown in Supporting Information Figure S2, where σ_i is initial conductivity of PAni, −5°C thin film (before immersion), while σ_f is time dependent conductivity of PAni, −5°C thin film after immersion in various concentration of hydrazine (1–100 ppm). Among all PAni films, PAni, −5°C exhibited the highest sensitivity to hydrazine. The differences in the responses and sensitivities could be attributed to the difference in the molecular weight and structure of PAni achieved from different polymerization temperature.[33,45] Those with high molecular weight and less defect sites encourage better doping process, and subsequently better dedoping process during reaction with hydrazine. PAni, −5°C which have the most active sites (doped sites) and increased molecular weight with less defect sites due to the sub-zero polymerization temperature[54] is able to interact rapidly with hydrazine and readily undergo conversion from ES state (high conductivity) to LE state (low conductivity).[55]

FTIR Measurement

Supporting Information Figure S3 shows the FTIR spectroscopy of (a) PAni, −5°C before immersion and (b) after immersion in 1 ppm of hydrazine. This is important to validate the structural changes that took place during the immersion of PAni, −5°C thin film in hydrazine. The intensity ratio of quinoid (Q) to benzenoid (B) (I_Q/I_B) are taken into account to justify the extent of oxidation state of PAni, −5°C, which resembles the availability of the quinoid diimine and benzene ring structure in the PAni, −5°C backbone.[56,57] The I_Q/I_B ratio of the PAni, −5°C film has decreased from 1.0 to 0.91 after the immersion. The result is in agreement with the dedoping reaction which took place during the immersion.[58,59]

Interaction of PAni with Hydrazine

Typically, PAni, −5°C is suitable to be used as sensing material as it could exhibit different oxidation states when exposed to base, reducing and/or oxidizing agents. Based on the reported UV–Vis, conductivity and FTIR measurements, we have proposed the possible interaction that took place during the immersion of PAni, −5°C thin film into the hydrazine solution in Scheme 1. Before immersion in hydrazine, PAni, −5°C in the ES state possesses both benzenoid and quinoid structures together with free charge carriers which give rise to the polaron absorbance at ~775–786 nm and high conductivity. During immersion, hydrazines (hydrazinium $[N_2H_5]^+$ ions) tend to wash away the AOT^- dopants from the ES backbone. Subsequently, electron re-arrangement takes place to produce PAni, −5°C with predominating benzenoid units and LE is formed which results in depreciation of polaron absorbance and conductivity values. PAni, −5°C could serve as an effective hydrazine sensor as the half oxidized state of ES can be reduced to LE upon exposure to hydrazine.[55]

CONCLUSION

In this study, PAni chemical sensors with different polymerization temperatures (−10, −5, 0, and 25°C) were prepared via chemical oxidative polymerization. Based on our knowledge, this simple and cost-effective PAni sensor set-up for hydrazine detection is novel and is being reported for the first time. PAni thin film was used for hydrazine detection in the concentration range from 0.05 to 5.00 ppm which showed a tolerable limit of detection of 0.24 ppm and lower when compared to the standard set by OSHA. PAni, −5°C could exhibit significant response to hydrazine in as fast as 0.12 min (7 s). Thus, preparation of PAni, −5°C is highly recommended as an effective chemical

sensor in hydrazine detection with shortest response and recovery time of 0.12 min (7 s) and 0.08 min (5 s), respectively with good reusability up to 10 cycles.

ACKNOWLEDGMENTS

The authors would like to show high gratitude for the financial support of this research by University of Malaya Research Grant (UMRG) (RG271/13AFR), ERGS (ER003/2012A), PPP (PV043/2012A), and ministry of higher education (MoHE) for the scholarships. Authors also would like to thank Dr. Desmond Ang Teck Chye for the English correction of this manuscript.

REFERENCES

1. Zeghina, S.; Wojkiewicz, J. L.; Lamouri, S; Belaabed, B.; Redon, N. *J. Appl. Polym. Sci.* **2014**, 40961.
2. Karyakin, A. A.; Lukachona, L. V.; Karyakina, E. E.; Orlov, A. V.; Kappachora, G. P. *Anal. Commun.* **1999**, *36*, 153.
3. Tripathi, A; Misra, K. P.; Shukla, K. *J. Appl. Polym. Sci.* **2013**, *130*, 1941.
4. Ahmad, N.; MacDiarmid, A. G. *Synth. Met.* **1996**, *78*, 103.
5. Rose, T. L.; Antonio, S. D.; Jilson, M. H.; Kron, A. B.; Suresh, R.; Wang, F. *Synth. Met.* **1997**, *85*, 1439.
6. MacDiarmid, A. G. *Synth. Met.* **1997**, *84*, 27.
7. Campos, M.; Miziara, T. A. S.; Cristovan, F. H.; Pereira, E. C. *J. Appl. Polym. Sci.* **2014**, *131*, 40688.
8. Wang, X.; Shao, M.; Shao, G.; Wu, Z.; Wang, S. *J. Colloid Interf. Sci.* **2009**, *332*, 74.
9. Umar, A.; Rahman, M. M.; Kim, S. H.; Han, Y. B. *Chem. Commun.* **2008**, *2*, 166.
10. Golabi, S. M.; Zare, H. R. *J. Electroanal. Chem.* **1999**, *465*, 168.
11. Choudhary, G.; Ilansen, H.; Donkin, S.; Kirman, C. Toxicological profile for hydrazines; Agency for Toxic Substances and Diseases Registry, **1997**, p 1.
12. Umar, A.; Abaker, M.; Faisal, M.; Hwang, S. W.; Baskoutas, S.; Al-Sayari, S. A. *J. Nanosci. Nanotechnol.* **2011**, *11*, 3474.
13. Ibrahim, A. A.; Dar, G. N.; Zaidi, S. A.; Umar, A.; Abaker, M.; Bouzid, H.; Baskouts, S. *Talanta* **2012**, *93*, 257.
14. Ravichandran, K.; Baldwin, R. P. *Anal. Chem.* **1983**, *55*, 1782.
15. Kamyabi, M. A.; Shahabi, S.; Hosseini, M. H. *J. Electrochem. Soc.* **2008**, *155*, F8.
16. Maleki, N.; Safavi, A.; Tajabadi, F. *Anal. Chim. Acta* **2008**, *611*, 151.
17. Nassef, H. M.; Radi, A. E.; O'Sullivan, C. K. *J. Electroanal. Chem.* **2006**, *592*, 139.
18. Zare, H. R.; Nasirizadeh, N. *Electrochim. Acta* **2007**, *52*, 4153.
19. Zheng, L.; Song, J. F. *Sens. Actuat. B* **2009**, *135*, 650.
20. Kiattiburr, P.; Tarachiwin, L.; Ruangchuan, L.; Sirivat, A.; Schwank, J. *React. Funct. Polym.* **2002**, *53*, 29.
21. Epstein, A. J.; Ginder, J. M.; Zuo, F.; Bigelow, R. W.; Woo, H. S.; Tanner, D. B.; Richter, A. F.; Huang, W. S.; MacDiarmid, A. G. *Synth. Met.* **1987**, *18*, 303.
22. Ping, Z. *J. Chem. Soc. Faraday Trans.* **1996**, *17*, 3063.
23. Rodrigues, P. C.; Cant, P.; Gomes, M. A. B. *Eur. Polym. J.* **2002**, *38*, 2213.
24. Park, O.-K.; Jeevananda, T.; Kim, N. H.; Lee, J. H. *Scripta Mater.* **2009**, *60*, 551.
25. Choudhury, A. *Sens. Actuat. B* **2009**, *138*, 318.
26. Quillard, S.; Louarn, G.; Buisson, J. P.; Boyer, M.; Lapkowski, M.; Pron, A. *Synth. Met.* **1997**, *84*, 805.
27. Sedenkova, I.; Trchova, M.; Stejskal, J. *Polym. Degrad. Stabil.* **2008**, *93*, 2147.
28. Wei, Y.; Hsuech, F. K.; Jang, G. W. *Macromolecules* **1994**, *27*, 518.
29. MacDiarmid, A. G.; Epstein, A. J. *Synth. Met.* **1994**, *65*, 103.
30. Kim, B. J.; Oh, S. G.; Han, M. G.; Im, S. S. *Synth. Met.* **2001**, *122*, 297.
31. Athawale, A.; Kulkakarni, M. V.; Chabukswar, V. V. *Mater. Chem. Phys.* **2002**, *73*, 106.
32. Xia, H.; Wang, Q. *J. Nanopart. Res.* **2001**, *3*, 399.
33. Yang, D.; Lu, W.; Goering, R.; Mattes, B. R. *Synth. Met.* **2009**, *159*, 666.
34. Blaha, M.; Varga, M.; Prokes, J.; Zhigunov, A.; Vohlidal, J. *Eur. Polym. J.* **2013**, *49*, 3904.
35. Li, Q.; Cruz, L.; Philips, P. *Phys. Rev. B* **1993**, *47*, 1840.
36. Gemeay, A. H.; Mansour, I. A.; El-Sharkawy, R. G.; Zaki, A. B. *Eur. Polym. J.* **2005**, *41*, 2575.
37. Stejskal, J.; Riede, A.; Hlavat, D.; Proke, J.; Helmstedt, M.; Holler, P. *Synth. Met.* **1998**, *96*, 55.
38. Wu, T. M.; Lin, Y. W.; Liao, C. S. *Carbon* **2005**, *43*, 734.
39. Chaudhari, H. K.; Kelkar, D. S. *Polym. Int.* **1997**, *42*, 380.
40. Trchová, M.; Šeděnková, I.; Konyushenko, E. N.; Stejskal, J.; Holler, P.; Marjanović, G. Ć. J. *Phys. Chem. B* **2006**, *110*, 9461.
41. Amrithesh, M.; Aravind, S.; Jayalekshmi, S.; Jayasree, R. S. *J. Alloy. Compd.* **2008**, *449*, 176.
42. Jiang, H.; Geng, Y.; Li, J.; Wang, F. *Synth. Met.* **1997**, *84*, 125.
43. Malinaukas, A.; Holze, R. *J. Electroanal. Chem.* **1999**, *461*, 184.
44. Salvatierra, R. V.; Oliveira, M. M.; Zarbin, A. J. G. *Chem. Mater.* **2010**, *22*, 5222.
45. Tai, H.; Jiang, Y.; Xie, G.; Yu, J.; Chen, X.; Ying, Z. *Sens. Actuat. B* **2008**, *129*, 319.
46. Raut, B. T.; Chougule, M. A.; Nalage, S. R.; Dalavi, D. S.; Mali, S.; Patil, P. S.; Patil, V. B. *Ceram. Int.* **2012**, *38*, 5501.
47. Conceição, C. D. C.; Faria, R. C.; Fatibello-Filho, O.; Tanaka, A. A. *Anal. Lett.* **2008**, *41*, 1010.
48. Liu, B.; Liu, Q.; Shah, M.; Wang, J.; Zhang, G.; Pang, Y. *Sens. Actuat. B* **2014**, *202*, 194.
49. Raoov, M.; Mohamad, S.; Abas, M. R.; Surikumaran, H. *Talanta* **2014**, *130*, 155.

50. Shankaran, D. R.; Narayanan, S. S. *Russ. J. Electrochem.* **2001**, *37*, 1149.

51. Ensafi, A. A.; Naderi, B. *Microchem. J.* **1997**, *56*, 269.

52. Ameen, S.; Akhtar, M. S.; Shin, H. S. *Talanta* **2012**, *100*, 377.

53. Ameen, S.; Akhtar, M. S.; Shin, H. S. *Sens. Actuat. B* **2012**, *173*, 177.

54. Geethalakshmi, D.; Muthukumarasamy, N.; Balasundaraprabhu, R. *Opt. - Int. J. Light Electron Opt.* **2014**, *125*, 1307.

55. Virji, S.; Kaner, R. B.; Weiller, B. H. *Chem. Mater.* **2005**, *17*, 1256.

56. Furukawa, Y.; Ueda, F.; Hyodo, Y.; Harada, I. *Macromolecules* **1988**, *21*, 1297.

57. Cataldo, F.; Maltese, P. *Eur. Polym. J.* **2002**, *38*, 1791.

58. Choi, B. G.; Park, H. S.; Im, H. S.; Kim, Y. J. *J. Membr. Sci.* **2008**, *324*, 102.

59. Yoon, S. B.; Yoon, E. Y.; Kim, K. B. J. *Power Sources* **2011**, *196*, 10791.